

## DIFFRACTIVE FRAGMENTATION IN HIGH ENERGY PHOTON REACTIONS

D. FRIES

### Introduction

I would like to discuss the subject of my talk in three parts;  
I intend:

- 1.) to review some aspects of inelastic reactions in general, and of diffractive inelastic reactions in particular.
- 2.) to present experimental evidence for a  $\xi^0$  signal in inelastic photon reactions which has a similar energy dependence between 4 and 18 GeV as the diffractive "elastic"  $\xi$  photo production.
- 3.) to discuss some relevant models which may provide an explanation of the effect.

## Experimental Information

The experimental data which were used for this study are film data from a multi-prong photo production experiment which was carried out by the SLAC Streamer Chamber (STC) group<sup>1</sup>. In this experiment the SLAC 2-meter Streamer Chamber was used to take pictures of hadronic multiprong photo production processes. We used a Bremsstrahlung photon beam of 18 GeV tip energy and a target of gaseous hydrogen. These - so far unpublished experimental data - are still being analysed; therefore, the results presented here are preliminary.

## Inelastic reactions at high energies

Inelastic reactions can be classified in two groups:

### I. quasi two body reactions of the type

$$a + b \rightarrow a^* + b^*$$

where  $a^*$  and  $b^*$  may be stable particle or some resonant states which decay. This reaction can be called "exclusive".

### II. general multiprong events of the type

$$a + b \rightarrow c + d + e + \dots$$

the reactions is being called "inclusive" when only one of the final state particles was observed.

Inelastic reactions in particular of the type II) have gained considerable interest in recent years as well from theoretical as from experimental point of view. One reason for this interest centers around the idea, that the nucleon may be made out of constituents. As possible candidates are being listed: Quarks, partons or bare conventional particles. One suspects that the general features of inelastic reactions at high energies

reflect the nature and the distribution of the fragments of the nucleon.

The field developed rapidly when SLAC experimentalists discovered that inelastic  $eP$  scattering at high energies showed unexpected features<sup>2</sup>: the data seem to be consistent with the idea that in inelastic electron scattering the virtual photon scatters from pointlike constituents of the proton, which have some momentum distribution and, according to models of Feynman, Bjorken and Paschos<sup>3</sup>, an average charge different from one. Their properties become visible under kinematical conditions where they can be treated just like a free gas; that is, at large  $x$ , where one defines

$$x = \frac{\nu}{q^2} \quad , \quad \text{"scaling" parameter}$$

$$\nu = E - E' \quad , \quad E, E' \text{ initial resp. final}$$

Electron energy

$$|q^2| \quad \text{four momentum transfer squared}$$

carried by the virtual photon

In fact Benreick et al.<sup>4</sup> have hypothesized that at high energies reactions such as



have the following general features in common: the distribution of kinematical quantities of the final state particles approach a limit at increasing energies. More concrete: the differential probability to observe a given momentum of a final state particle becomes independent of the incident energy. Since this property is due to a fragmentation of the target and/or of the projectile particle, one should observe it in the laboratory system or in the rest system of the incoming projectile respectively. Inelastic  $e p$  scattering serves as an example where the target fragmentation leads to a limiting

distribution. Experimentally one observes that

$$\lim_{E, E' \rightarrow \infty} \frac{d^2 \sigma}{dq^2 dM^{*2}} = \frac{2\pi \alpha^2}{M q^4} W_2(x)$$

the differential cross section for the excitation of any target mass  $M^*$  ( $M =$  proton mass) with a four momentum transfer  $q^2$ , reaches a limit independent of the energy of the incident electron. ( $\alpha =$  Fine structure constant.  $W_2(x) =$  Structure function)

There also exists now experimental information on a growing number of hadronic inelastic reactions which exhibit limiting distributions when viewed in the rest system of the target<sup>5</sup> (beam). Hence this may be interpreted as a consequence of the fragmentation of the target<sup>6</sup> of the projectile respectively.

#### Diffractive inelastic reactions

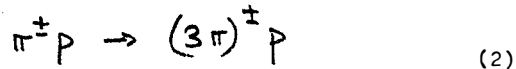
Inelastic reactions which are diffractionlike or show the pattern of diffraction dissociation constitute in the spirit of the fragmentation model just a special, restricted class;

- a) they have a limiting distribution in  $t$ , that is to say, the differential cross section  $\frac{d\sigma}{dt}$  becomes independent of the incident energy.
- b) the total quantum numbers  $I^2, G, I_z, N$  carried by fragments are those of the target (projectile)

In the usual language a) and b) are expressed by demanding that in diffraction dissociation the crossed channel can carry the Quantum numbers of the vacuum<sup>6</sup> (in case of a multiperipheral reaction one assumes that at least one  $t$  branch has this property).

Recent experimental evidence tends to confirm this point. For this some examples:

- 1.) It has been observed that in the reaction<sup>7</sup>



the 3 pion invariant mass accumulates in the mass region 1.0 - 1.3 GeV with very little dependence on the incident energy. Between 5 and 20 GeV/c incident momentum cross section and slope parameter appears to stay constant.

$$\begin{aligned} \sigma(3\pi) &= .5 \text{ mb} \\ R &= 9 (\text{GeV}/c)^2 \\ \ln \frac{d\sigma}{dt} &\sim \exp(-Rt) \end{aligned}$$

Thus a diffractive fragmentation of the projectile is indicated.

- 2.) Similarly an accumulation in the  $(P \ 2\pi)$  mass distribution was found in studying the reaction<sup>8</sup>



The cross section  $\sigma(P \ \pi^+ \ \pi^-)$  varied only slowly with energy when the invariant  $(P \ 2\pi)$  mass was in the region between 1.3 and 1.8 GeV. The cross section is about .5 mb at 25 GeV.

- 3.) Well known is diffractive Isobar production. Measurements of the total cross section of the reaction channel<sup>9</sup>



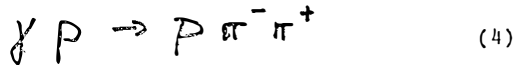
have been made between 4 and 30 GeV incident energy.  $N^*$ 's

which can be excited by the mere exchange of the natural spin parity series show diffractive behaviour. 1400 ( $1/2^+$ ), 1500 ( $3/5^-$ ), 1688 ( $5/2^+$ ), 2190 ( $7/2^-$ ). The  $\Delta(1236)$   $3/2^+$  which requires Isospin exchange has a cross section which falls off rapidly with energy. The cross sections are in the order of .5 mb. In Fig. 1 we plotted cross sections for  $N^*(1400)$ ,  $N^*(1688)$  and  $\Delta(1236)$  together with the total elastic P P cross section.

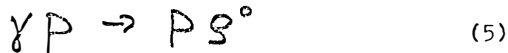
### Photoproduction of $\rho^0$ .

For photon induced hadronic processes at energies above 4 GeV the diffractive nature of the production processes for  $\rho^0$  mesons is experimentally well established<sup>10</sup>.

In addition the process



is at high energies almost completely saturated by the reaction channel



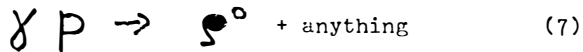
which illustrates very clearly the close affinity of photons and  $\rho^0$  Mesons. This is shown in Fig. 2 where the ratio

$$R = \frac{\gamma P \rightarrow P \rho^0}{\gamma P \rightarrow P \pi^- \pi^+} \quad (6)$$

was plotted. Hence we refer to the reaction (5) as to the "elastic"  $\rho^0$  photo production.

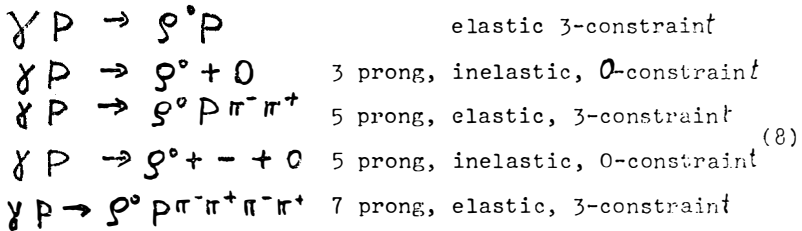
Because of the dominating coupling of the photon in the elastic reaction it would be very interesting to know something about the  $\gamma$ - $\rho$  coupling in inelastic reactions. With other words - referring to the fragmentation idea - , what happens to the  $\gamma$ - $\rho$  coupling when the target proton or the projectile fragmentizes ?

One can hope to obtain some information about this problem by studying the reaction



which one classifies as "inclusive" reaction.

Analysing the Streamer Chamber data we find as the main contributions of hadronic final states of the reaction (7) the following event types



+, -, 0 indicate the charges of the final state particles, where the masses are unknown. Thus the events fall apparently into two classes

- a) events, which satisfy energy and momentum conservation; they can be fitted by a three constraint fit (3C), which renders the identity of the masses of all final states.
- b) events, which do not satisfy energy and momentum conservation. We call them zero constraints (0C). The masses of the final state particles are not known.

We have neglected in the list (8) strange particle production and higher than 7 prong events and concentrated for this study on three prong and five prong events.

### Generalities of the Analysis

One realizes that it is difficult to analyse the class of the OC events, since we don't know the incident energy and have for those events no constraint to evaluate it.

In order to make as few assumptions as possible we proceed to analyse the OC events of the reaction (7) as follows

- 1) we classify the events into bins of visible energy  $E_c$   
 (for  $4 \leq E_c \leq 18$  GeV)

$$E_c \approx \sum |\vec{p}_i|_{\text{CHARGED}} \quad (9)$$

N = number of charged tracks

- 2) in order to isolate the  $g^0$  signal we compute the invariant mass of + - charged particles (all combinations) assuming that the particle mass was  $M_\pi$ . This must clearly be wrong for all "+" particles which were in fact protons and not  $\pi^+$ . However, we can expect that the wrong mass assignments contribute mainly to a general broad background in the two-particle invariant mass spectrum, on top of which the  $g^0$  signal should show up.
- 3) Instead of  $t$  which cannot be determined for OC events we propose to study the distribution of the Lorentz-Scalar quantity  $t'$ .

$$t' = \frac{t - M^2}{s - M_p^2} = \frac{-1}{M_p} (E_S - p_S \cos \theta_{\text{LAB}})$$

where  $M$ ,  $E_{\xi}$ ,  $P_{\xi}$ ,  $\theta_{\text{LAB}}$  is the mass resp. energy, momentum and production angle of the observed  $\xi^0$  in the LAB system.  $t'$  can therefore directly be measured.

- 4) Instead of the standard Helicity system (which is inaccessible without knowing  $S$ , the total CM energy) we choose to study the  $\xi$  decay angular distribution in a  $\xi^0$  testframe, where the direction of the  $\xi$  in the LAB system becomes the axis of quantisation. Both systems are connected by a rotation in the scattering plane. By computing the (rotational invariant) Eigenvalues of the Decay Density Matrix one can make comparisons.

## Results

The study of the inelastic  $\xi^0$  photo production is based on about 8000 3 prong and 7500 5 prong events having a visible energy  $E_c$  between 4 and 18 GeV <sup>\*</sup>. In selecting the inelastic  $\xi^0$  from the data two problems arise: 1) the separation of inelastic 3 prongs from the elastic 3 prongs, 2) the corrections due to detection and trigger efficiency of the STC and the absolute normalisation of the single rate.

A safe separation of the 3 prong 3C and 0C events was obtained by selecting with two cuts from the fit probability distribution. Events which fitted the energy momentum constraint with a probability greater than 1 % were taken as "elastic" (3C) events.

---

\* A complete account of the STC photo production experiment is to be published by the SLAC group in near future, who gave kind permission to discuss some of the preliminary results.

Those which have fit probabilities of  $10^{-6}$  or less were considered as "inelastic" (OC) events. (The uncertainty about the events inbetween was taken in account in estimating errors.) In computing ratios of inelastic and elastic rates for the same charge topology, most corrections such as the trigger-and detection efficiency, and also the absolute normalisation, factor and drop essentially out.

Classifying events into bin of  $E_c$  we have plotted the distribution of the invariant masses of the  $+ -$  charged particles, as it was described in the preceeding chapter. In Fig. 3 the elastic events are shown together with the inelastic events for 4 different energy bins. For OC 3 prongs we plotted the two possible mass combinations. The shaded part of the histogram represents the invariant mass spectrum of the two "+" particles.

One recognizes the dominant  $\varrho^0$  signal in the elastic events. Also in the OC events a strong  $\varrho^0$  signal can be recognized; it is accompanied by some structure in the region of lower  $\pi^+\pi^-$  masses. One can regard the  $++$  mass spectrum as a general random background representing phase base and the wrong mass assignments also for the  $+ -$  mass distribution. This exhibits the  $\varrho^0$  signal more clearly.

Most important is the observation that the relative strength of the  $\varrho^0$  signal of the OC events depends very little on the energy  $E_c$ . In fact the energy dependence seems to be not very different from the energy dependence of the diffractive "elastic"  $\varrho^0$  signal.

For 5 prongs the analysis is more complicated, because of the many possible  $+ -$  combinations. In Fig. 4 the 3 constraint and the 0-constraint events are shown again side by side for three

energy bins of  $E_c$ . In the 3C category 4 combinations have been plotted. A strong  $\varrho^0$  signal with about equal relative strength is present in all energy bins. In the 0C category one would have to plot six "+ -" mass combinations. In order to exhibit the presence of a  $\varrho^0$  signal on a smaller background we selected always that + - combination, which has the highest momentum  $|\vec{P}_{+-}|$ . Evidence of a  $\varrho^0$  signal is again visible in all energy bins. There is again some structure in the lower mass region.

Next we proceed to calculate ratios with respect to the elastic  $\varrho^0$  signal, fitting the mass spectrum in the  $\varrho$  region to a BreitWigner distribution and a smooth background or - when this rendered ambiguous results - performing a crude background subtraction by hand. Since the  $\varrho^0$  rates obtained this way can only be approximate, we assigned large errors in order to cover most of the systematic uncertainties. In spite of the uncertainties involved,\* however, one can clearly recognize (Fig 5) that the ratio of the elastic and the inelastic 3 prong events shows no major energy dependence. We obtained the rates of 5 prong (3C and 0C)  $\varrho^0$  in a similar fashion. Since again the ratio to the elastic  $\varrho^0$  rate appeared to be constant we combined the results of 3 and 5 prongs and plotted in Fig also the ratio of the rate of inelastic  $\varrho$ 's in 3 and 5 prongs to the elastic rate.

---

\* Forming ratios one has also to keep in mind that 0C and 3C events of the same visible energy  $E_c$  are produced by different photon energies  $E_\gamma$ , because of the missing energy of the neutral particles. Thus, there is an uncertainty in the energy scale as well.

Since the ratio's obtained this way seem to be energy independent and because one knows that the elastic  $\rho^0$  photo production is diffractive, we are led to believe that photon induced reactions at high energy contain a diffractive  $\rho^0$  signal which is of the order or greater than the elastic  $\rho$  cross section.

### Discussion.

Following our earlier discussion, the experimental observation indicates a diffractive fragmentation of the target or/and of the projectile. The projectile consisting of an isoscalar and an isovector photon could fragmentize diffractively into an odd respectively even number of pions.

This study shows evidence of a diffractive fragmentation of the isovector photon simultaneously with a fragmentation of the target. In particular one can think of the following

- 1.) In a recent study, G. Wolf<sup>11</sup> parametrized diffractive inelastic  $\rho$  photo production in terms of peripheral diagrams. Specifically the contribution of diffractive Isobar production and double peripheral scattering has been estimated.

The possibility to factorize the residue functions in the Regge Model permits one to relate processes which have one vertex in common; thus the following relation has been used:

$$\frac{\frac{d\sigma}{dt}(\gamma P \rightarrow \rho^0 P)}{\frac{d\sigma}{dt}(\gamma P \rightarrow \rho^0 N^*)} = \frac{\frac{d\sigma}{dt}(PP \rightarrow PP)}{\frac{d\sigma}{dt}(PP \rightarrow PN^*)} \quad (9)$$



2.) A very interesting mechanism could link the inelastic  $g^0$  photo production to inelastic e P scattering. Bjorken and Paschos have discussed the similarity of inelastic eP scattering and inelastic Compton scattering in the frame work of the parton model. They derived the following result which should hold in the deep inelastic region

$$\frac{2EE'}{v^2} \frac{d^2\sigma}{d\Omega dk'} (\gamma p)^{incl} = \frac{\langle \sum Q_i^4 \rangle}{\langle \sum Q_i^2 \rangle} \quad (11)$$

where  $k'$ ,  $E'$  are the energies of the outgoing photon resp. electron.  $\langle \sum Q_i^4 \rangle$  is the average squared charge of a parton.  $v = E - E'$ , and  $E$  is the energy of the incident electron. One notes that (11) states that the ratio of the two reactions times a kinematical factor is a constant. (11) could be used to determine this constant and therefore the average parton charge.

Now inelastic Compton scattering at high energies - especially if only Bremsstrahl photon beam is available - is experimentally a very unattractive reaction (How can one isolate the final photon amongst all the  $\gamma$ 's coming from  $\pi^0$  decay). However, if the final photon in the inelastic Compton process converts into a  $g^0$  the "projectile" could be observed in the final state. In fact, this final state should be part of the final state of the reaction (7) which we investigate.

the rate of the process  $\gamma p \rightarrow \gamma + \text{anyth.}$  would be reduced by a factor

$$\alpha (f_\rho^2 / 4\pi)^{-1} \approx 0.4 \times 10^{-3}$$

neglecting finite width corrections for the  $\rho$  mass and using the vector dominance idea, where  $\alpha$  is the fine structure constant and  $f_\rho^2 / 4\pi$  is the photon- $\rho$  coupling constant.

The question whether relation (11) can be tested using the SLAC STC data is presently being studied.

### Conclusion

Using preliminary results of the SLAC Streamer chamber group, we presented evidence for diffraction fragmentation in  $\gamma p$  processes. More detailed investigations concerning the  $\rho$  decay angular and the momentum distribution are not yet completed.

### Acknowledgements

I am indebted to my colleagues from the SLAC STC group for letting me discuss the STC data prior to publication.

## References

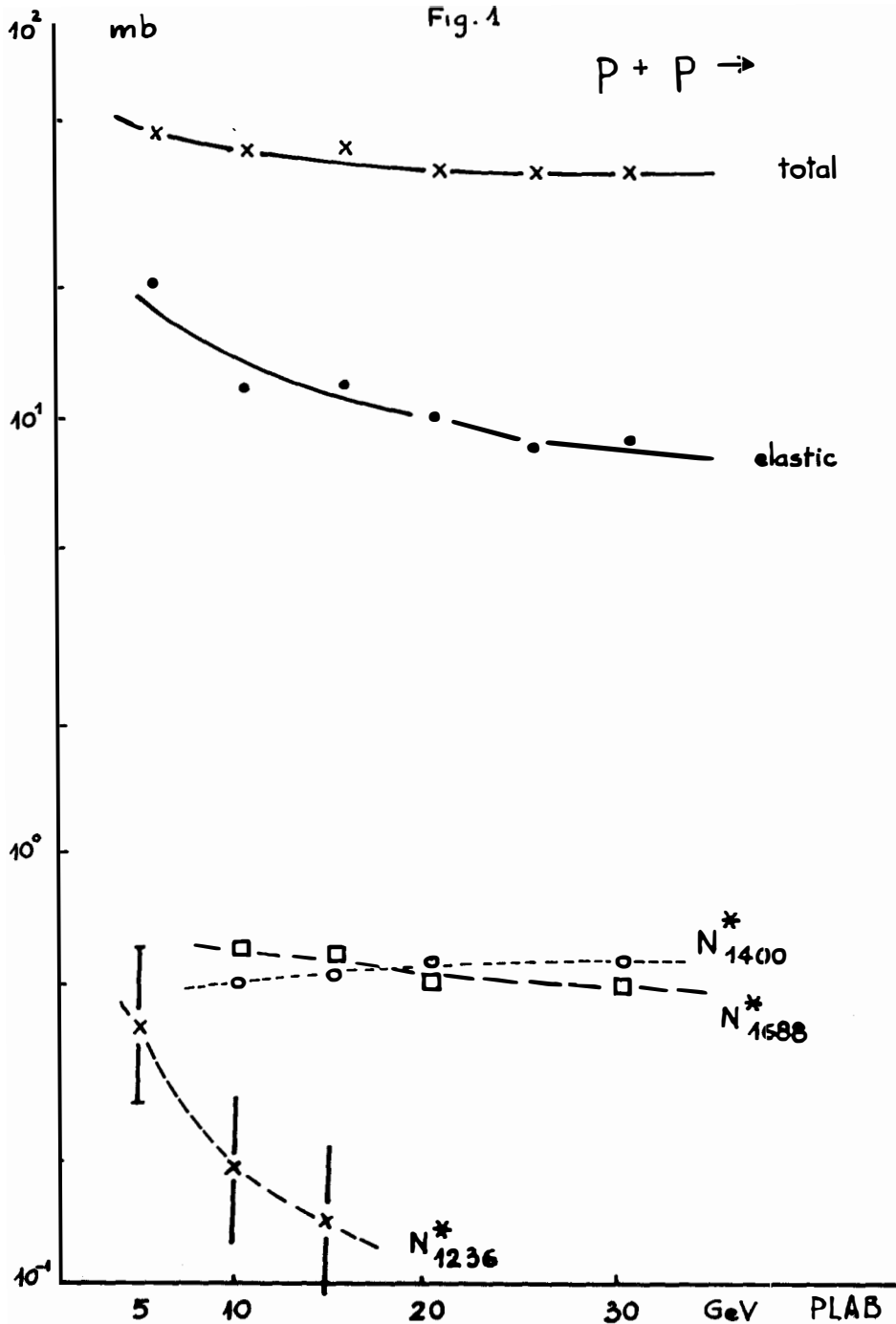
- 1.) SLAC Streamer Chamber group (1969)  
M. Davier, I. Derado, D. Fries, M. Liu, R. Mozley  
A. Odian, J. Park, W. Swanson, F. Villa and D. Yount.
- 2.) A recent review is given by F.J. Gilman SLAC-PUB-842  
Nov. 1970
- 3.) J.D. Bjorken, E.A. Paschos, Phys. Rev. 185, 1975 (1969)  
R.P. Feynman talk given 1965 at Stony Brook conference  
Sept. 1969 "High Energy Collisions"  
C.N. Yang et al. Gordon and Breach 1969
- 4.) J. Benecke, T.T. Chou, C.N. Yang and E. Yen  
Phys. Rev. 188, 215, (1969)
- 5.) See for example R.W. Anthony, C.T. Coffin, E.S. Meanley, K.M. Terwilliger  
and N.R. Stanton  
Phys. Rev. Lett. 26, 38 (1970)
- 6.) F. Zachariasen, CERN TH-1284 (1971)
- 7.) G. Ascoli et.al. Phys. Rev. Lett. 21, 113, (1968)
- 8.) R.A. Jespersen et.al. Phys. Rev. Lett. 21, 1368 (1968)  
R. Ehrlich et.al. Phys. Rev. Lett. 21, 1839 (1968)
- 9.) Anderson et.al. Phys. Rev. Lett. 16, 855, (1966)
- 10.) see f. example G. Wolf DESY report 70/64 Dec. 1970
- 11.) G. Wolf 'On inelastic diffractive Rho photoproduction and  
and Compton Scattering'  
DESY Aug. 1970 (unpublished)

Figure Captions.

---

- Fig. 1 P P reactions , total cross section, elastic cross section, total cross section for the reaction channels  
 $P P \rightarrow P N^*$  1400  
 $P P \rightarrow P N^*$  1688
- Fig. 2 The ratio  $\frac{\gamma P \rightarrow \rho^0 P.}{\gamma P \rightarrow P \pi^+ \pi^-}$   
as a function of photonenergy
- Fig. 3 Invariant  $\pi^+ \pi^-$  Mass spectrum for 3-constraint and 0-con-  
straining 3 prong events  
shaded area:  $\pi^+ \pi^+$  Mass spectrum
- Fig. 4 Invariant  $\pi^+ \pi^-$  Mass spectrum for 3-constraint and 0-con-  
straint 5 prongs.  
3 C : 4 combinations of +-particles  
0 C: one combination with max  $|\vec{P}_+|$  selected
- Fig. 5 ratio of inelastic  $\rho^0$  production over elastic (3 prong)  
 $\rho^0$  production as a function of  $E_{\text{charged}}$

Fig. 1



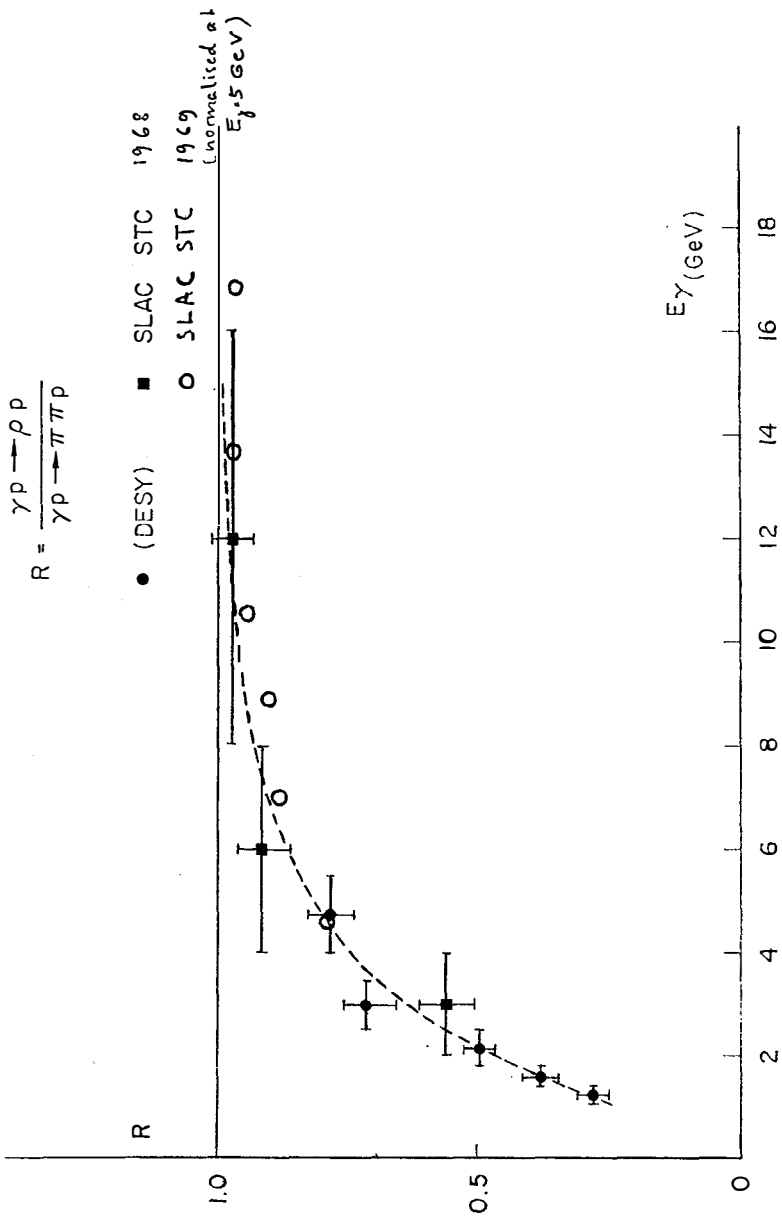


Fig. 2

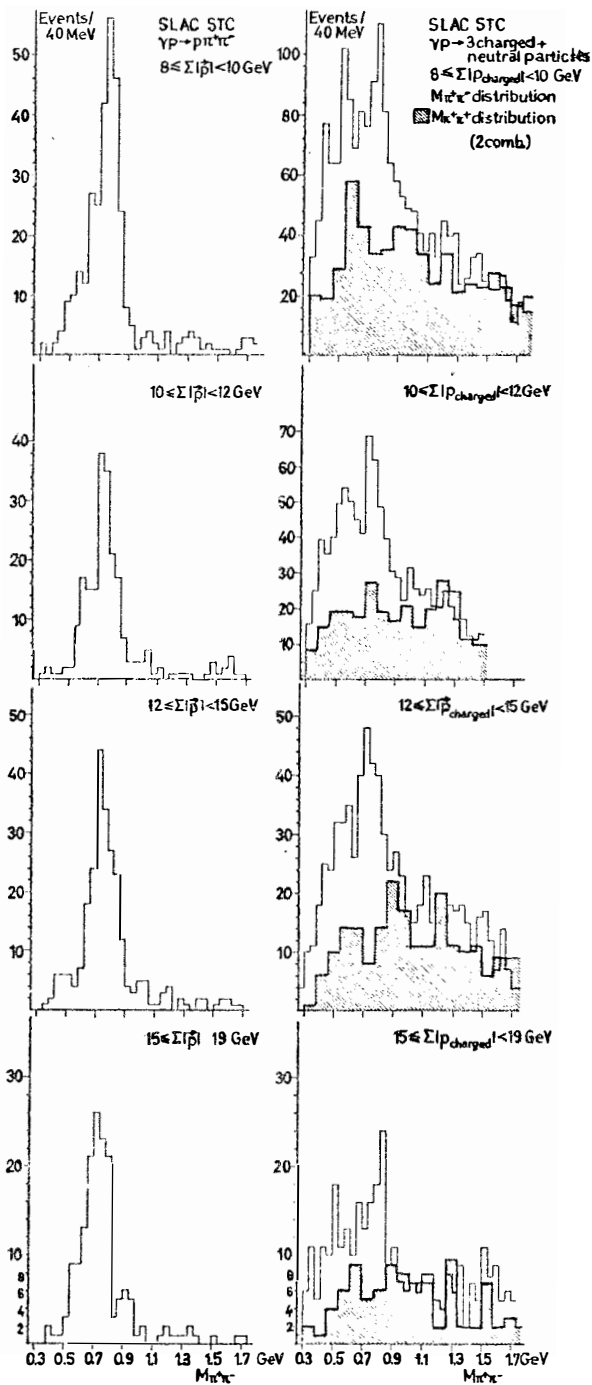
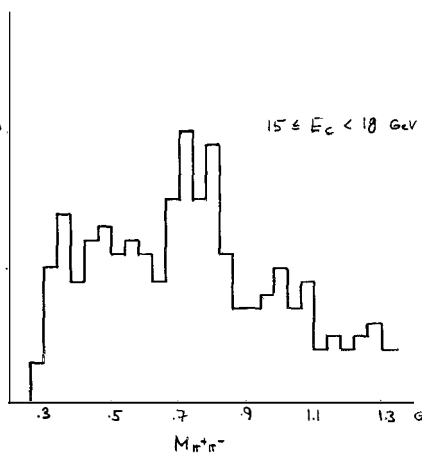
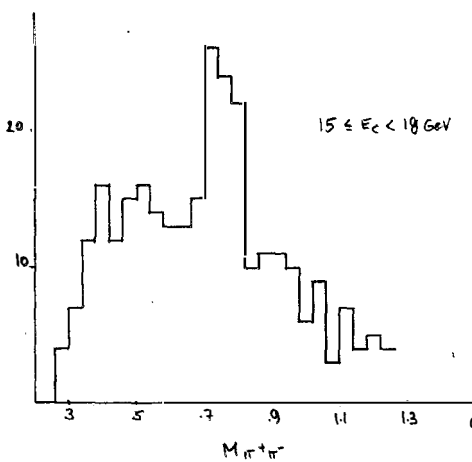
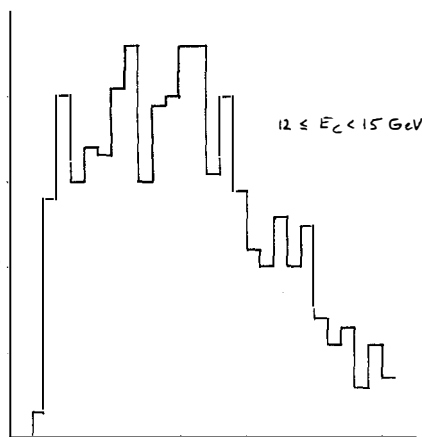
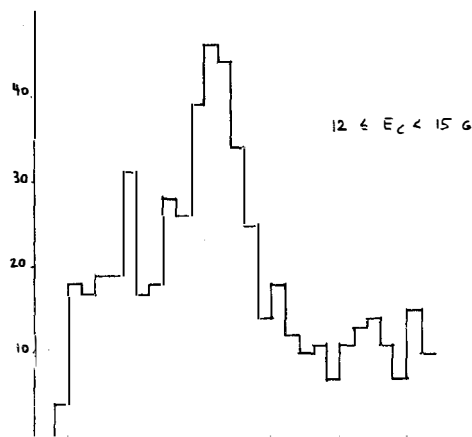
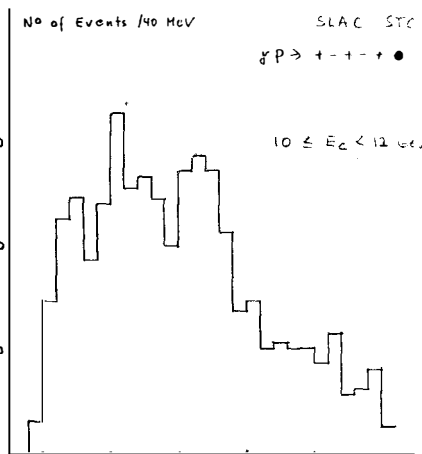
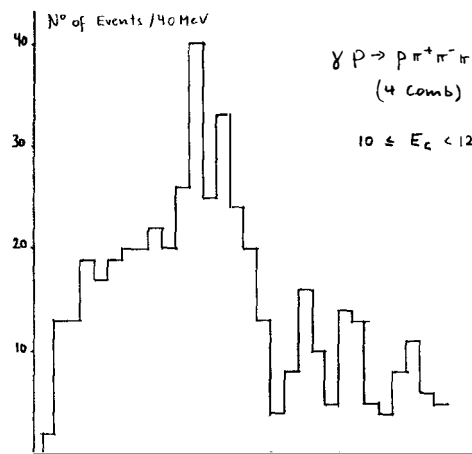


Fig. 3



$M_{\pi^+ \pi^-}$

$M_{\pi^+ \pi^-}$

Fig. 4

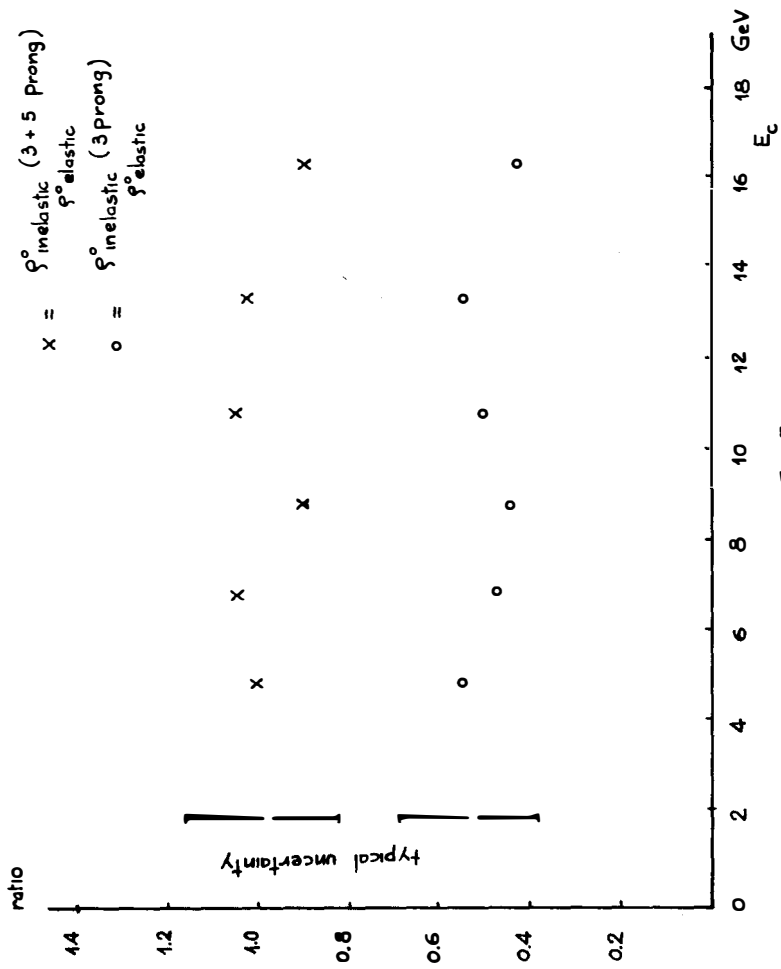


Fig. 5